

A MEMORY-EFFICIENT DISTRIBUTED ALGORITHM FOR APPROXIMATE NEAREST NEIGHBOUR SEARCH WITH ARBITRARY DISTANCES

A PREPRINT

 **Elena García-Morato***
CETINIA-DSLAB
Universidad Rey Juan Carlos
Madrid, Spain
elena.garciamorato@urjc.es

 **Felipe Ortega**
CETINIA-DSLAB
Universidad Rey Juan Carlos
Madrid, Spain
felipe.ortega@urjc.es

 **Maria Jesús Algar**
CETINIA-DSLAB
Universidad Rey Juan Carlos
Madrid, Spain
mariajesus.algar@urjc.es

 **Javier Gomez**
CETINIA-DSLAB
Universidad Rey Juan Carlos
Madrid, Spain
javier.gomez@urjc.es

 **Cesar Alfaro**
CETINIA-DSLAB
Universidad Rey Juan Carlos
Madrid, Spain
cesar.alfaro@urjc.es

 **Javier M. Moguerza**
CETINIA-DSLAB
Universidad Rey Juan Carlos
Madrid, Spain
javier.moguerza@urjc.es

January 15, 2026

ABSTRACT

Approximate nearest neighbour (ANN) search has become a central task in modern data-intensive applications, particularly when operating on large, heterogeneous, or high-dimensional datasets. However, many existing ANN methods struggle in such scenarios, either because they rely on metric assumptions or because their indexing strategies are not well suited to distributed environments or to settings with constrained memory resources. This work introduces PDASC (Parametrizable Distributed Approximate Similarity Search with Clustering), a distributed ANN search algorithm whose index design simultaneously supports arbitrary dissimilarity functions and efficient deployment in distributed, storage-aware environments. PDASC builds a distributed hierarchical index based on clustering mechanisms that are agnostic to distance properties, thereby accommodating non-metric and domain-specific similarities while naturally partitioning indexing and search across multiple computing nodes, with a compact per-node memory footprint. By preserving locally informative neighbourhood structure, the proposed index mitigates practical manifestations of the curse of dimensionality in high-dimensional spaces. We analyse how the index structural parameters govern the trade-offs among recall, computational cost, and memory usage. Experimental evaluation across multiple benchmark datasets and distance functions shows that PDASC achieves competitive accuracy–efficiency trade-offs while consistently requiring lower per-node memory compared to state-of-the-art ANN methods. By avoiding reliance on specialised hardware acceleration, PDASC enables scalable and energy-efficient similarity search in heterogeneous and distributed settings where memory efficiency and distance-function flexibility are first-class constraints.

Keywords Approximate Nearest Neighbour (ANN) search · Distributed Similarity Search · Hierarchical Clustering · High-Dimensional Data · Non-metric Distance Functions

1 INTRODUCTION

Searching for data objects that are close to a given query according to a similarity measure, typically formalised as a distance function, is a core task in today’s data-driven landscape, commonly referred to as similarity search [1, 2, 3].

*Corresponding author. This article is currently under peer-review.

This search paradigm underpins a wide range of fields, including information retrieval [4], content-based multimedia search [5], machine learning [6], bioinformatics [7], and cybersecurity [8].

A particularly important instance of this paradigm is the k -nearest neighbours (k -NN) search problem, in which the objective is to retrieve the k most similar objects to a given query according to the same dissimilarity function. A naive approach to k -NN search consists of computing the distance between the query and every element in the dataset, then selecting the k elements with the smallest distances. While this exhaustive search guarantees exact results, it quickly becomes computationally prohibitive as the dataset grows in size or dimensionality. Even indexing-based exact methods [3] suffer severe performance degradation in high-dimensional spaces, often yielding negligible efficiency gains over a full scan due to the *curse of dimensionality* [9]. To address these limitations, Approximate Nearest Neighbour (ANN) search has emerged as a practical alternative, relaxing strict accuracy requirements in exchange for substantial efficiency gains.

Beyond these classical high-dimensional challenges, modern data science introduces additional sources of complexity, as datasets with heterogeneous features, outliers, and distributed storage are increasingly prevalent. Recent studies [10, 11, 12] have explored the use of alternative distance measures for similarity search in spaces with diverse topologies, showing that non-conventional distance functions may better capture similarity between elements and can strongly influence ANN performance. However, many existing exact or approximate similarity search methods were originally designed for metric or centralised settings, limiting their applicability in such modern contexts. These emerging requirements motivate similarity search approaches that support arbitrary distance functions and scale effectively across distributed infrastructures.

Building on these considerations, we propose PDASC (Parametrizable Distributed Approximate Similarity Search with Clustering), a fully distributable ANN search algorithm capable of operating under a wide range of distance functions. PDASC constructs an index structure tailored to distributed environments through an unconventional application of hierarchical clustering. This enables scalable search while supporting a broad spectrum of dissimilarity measures (including non-metric, asymmetric, and learned distances), while providing competitive performance without relying on hardware acceleration strategies such as GPUs or TPUs.

In summary, the main contributions of this research are:

- We introduce PDASC, a natively distributed ANN search algorithm that supports a broad range of distance functions and is designed to operate effectively on high-dimensional and heterogeneous data.
- We study how PDASC’s tailored use of hierarchical clustering mitigates several practical manifestations of the *curse of dimensionality* and how the induced index topology governs efficiency, memory usage, accuracy, and pruning dynamics. We further show how structural parameters determine the underlying trade-offs.
- We conduct an extensive empirical evaluation, assessing PDASC across multiple benchmark datasets under various distance functions and comparing it with state-of-the-art ANN algorithms from different families, such as ANNOY, PyNNDescent, LSH, IVF and HNSW. Experiments demonstrate its robustness in distributed environments and its competitive efficiency relative to established methods.

The paper is organised as follows. Section 2 formalises our problem statement and related work. Section 3 describes the PDASC algorithm, and Section 4 details the empirical evaluation conducted on benchmark datasets and presents the corresponding findings. Finally, section 5 summarises the main contributions of this paper and discusses further directions for future work.

2 BACKGROUND AND RELATED WORK

2.1 SIMILARITY SEARCH

Building on the definition introduced in Section 1, similarity search can be formally defined over a dataset of objects \mathbb{X} , each represented as a feature vector in a multidimensional space, together with a dissimilarity function $\delta : \mathbb{X} \times \mathbb{X} \rightarrow \mathbb{R}$ that quantifies how different two objects $a, b \in \mathbb{X}$ are by assigning a numerical score $\delta(a, b)$. Larger values of $\delta(a, b)$ indicate greater dissimilarity, whereas smaller values correspond to more similar objects. Given a query object $q \in \mathbb{X}$, the goal of this paradigm is to identify the object $o \in \mathbb{X}$ or, more generally, a subset $S \subseteq \mathbb{X}$, that minimises $\delta(q, o)$.

Within this framework, two main retrieval tasks are commonly distinguished: the k -NN search and the *range query*. The k -NN search retrieves the subset of k objects in the database that are closest to the query q according to the dissimilarity measure δ , i.e., the k elements $o_i \in \mathbb{X}$, where $i = 1, \dots, k$, with the smallest values of $\delta(q, o_i)$. In turn, the range query returns all objects whose distance from the query does not exceed a predefined radius r , namely those $o_i \in \mathbb{X}$ such that

$\delta(q, o_i) \leq r$. The computational cost of similarity search queries primarily arises from comparing a query object with a large collection of high-dimensional feature vectors in order to determine their similarity, which requires numerous evaluations of the dissimilarity function $\delta(a, b)$ [2]. In similarity search, these queries can be addressed either in an *exact* or *approximate* manner.

Exact methods guarantee the retrieval of the complete and correct result set, such as all true nearest neighbours or all elements within a specified range, even at the cost of evaluating every distance. Approximate methods, in contrast, trade a small degree of accuracy for substantial gains in efficiency, either by reducing the number of distance computations (NDC) or by exploiting compact indexing structures.

However, exact methods are limited in their effectiveness in high-dimensional spaces, which are affected by phenomena such as the *empty space problem* [1] and *measure concentration* [13]. As dimensionality increases, the volume of the space grows exponentially, whereas the point density decreases. This makes distances become increasingly concentrated, with the relative difference between nearest and farthest neighbours shrinking and thereby diminishing the meaning of proximity, a phenomenon commonly referred to as the *curse of dimensionality* [9]. Empirical studies show that, under these conditions, the performance of exact k -NN search methods degrades to that of a sequential scan [14]. This motivates the use of approximate search methods, which aim to maintain efficiency in high-dimensional spaces while providing sufficiently accurate results for practical purposes.

2.2 ANN SEARCH

Following the exact k -NN formulation (see Section 2.1), the objective of ANN search is to retrieve the k elements of \mathbb{X} that best approximate the true nearest neighbours of q under the dissimilarity function δ , thereby relaxing strict accuracy requirements in exchange for significant efficiency gains.

ANN methods typically operate in two distinct phases: an index-building phase and a search phase. During the index-building phase, the dataset is mapped into a so-called index data structure tailored to enable efficient exploration of the search space. These index structures can be broadly classified into several families, including methods based on geometric partitioning [15, 3], proximity graphs [16, 17], hashing functions [18, 19], clustering [20], vector quantisation [21, 22], permutation-driven schemes [23, 24], and, more recently, learned and hybrid indices [25, 26].

During the search phase, ANN methods exploit the inherent structural properties of the index to constrain the portion of the search space to be examined, thus reducing the number of candidate elements to evaluate. Some approaches achieve this implicitly through their algorithmic design. For example, graph-based indices guide the search via greedy or heuristic traversals on a proximity graph. In contrast, hashing-based techniques exploit the distribution of collisions in the hash spaces. Others rely on explicit pruning rules to further limit the search space. In metric settings, several of these pruning rules are relaxed or heuristic variants of geometric strategies originally developed for exact search. For instance, the triangle inequality has traditionally been employed to derive distance bounds from previously computed distances to reference elements, effectively excluding regions that cannot contain closer neighbours [3]. However, such pruning strategies are not universally applicable: methods that operate with arbitrary or non-metric dissimilarity functions cannot reliably exploit geometric properties to guide the search.

2.3 NON-METRIC DISTANCE FUNCTIONS ON ANN SEARCH

Although exact nearest-neighbour search in high-dimensional Euclidean spaces is also computationally expensive [27, 28], Euclidean distance remains widely used in indexing structures and search algorithms [29]. This situation has motivated an increasing exploration of alternative, non-metric distance functions in high-dimensional ANN applications.

Firstly, many practical similarity measures used in domains such as text, vision, speech, and recommender systems (e.g., cosine-based distances, Kullback-Leibler and Jensen-Shannon divergences, or learned similarity functions) are inherently non-metric and often capture domain-specific relationships more effectively than classical metric distances. In recent years, several studies [10, 11, 12] have examined the use of alternative distance measures for similarity search in spaces with diverse topologies, highlighting that selecting an appropriate dissimilarity measure can exert a significant impact on the performance of k -NN algorithms.

Secondly, high dimensionality can also lead to distance concentration, a phenomenon in which the variance of pairwise distances approaches zero as dimensionality increases, greatly reducing the effectiveness of metric-based pruning and undermining the efficiency of traditional exact indexing structures. Although recent advances in exact approaches [30] have improved the efficiency of exact k -NN search, these improvements do not fully compensate for the fact that exact methods become computationally impractical in high-dimensional spaces. In contrast, ANN methods remain operationally viable precisely because, as they do not depend on strict metric properties and can

accommodate weak, noisy, or inherently non-metric similarity functions, they are considerably less affected by the *curse of dimensionality* [27, 31].

Taken together, these observations highlight the need for flexible ANN methods that can seamlessly operate with multiple distance functions. In the following section, we build upon these insights to introduce our approach, which directly addresses these challenges.

3 THE PROPOSED ALGORITHM

In this work, we present PDASC, a fully distributable ANN search algorithm capable of operating under a wide range of distance functions. Our approach relies on applying conventional clustering techniques in a tailored manner to construct a hierarchical index specifically designed to address the challenges inherent to high-dimensional spaces. Its coarse-to-fine organisation progressively isolates local neighbourhoods in which distance relationships remain informative, even when global contrast collapses.

One key design choice in our method is the use of a relatively large number of prototype points to characterise each group at a given level of the hierarchy (typically 20–30% of the items in that group). This strategy is motivated by well-established manifestations of the *curse of dimensionality* (see Section 2): as dimensionality increases, global distances tend to concentrate and lose discriminative power, making them unreliable as sources of global information, whereas local geometric relationships remain meaningful. By selecting a larger set of prototypes to represent a group of points (cluster), PDASC preserves local neighbourhood structure, stabilises clusters, and improves separability at higher levels of the hierarchy. In practice, this yields a denser and more faithful partitioning of the space, making the index less sensitive to distance concentration and enabling more robust behaviour in high-dimensional settings.

Furthermore, by relying on clustering methods compatible with non-metric and domain-specific distance functions, PDASC can operate directly on heterogeneous data, thereby extending its applicability across diverse domains. In addition, its ability to support a wide range of distance functions makes it particularly useful in scenarios where the most appropriate similarity measure is not readily determined.

3.1 PDASC

At its core, PDASC operates in two phases: the Multilevel Structure Algorithm (MSA) for building the index, and the Neighbours Search Algorithm (NSA) for processing queries.

As outlined in Algorithm 1, MSA follows a bottom-up strategy to construct a multilevel index structure tailored for distributed, scalable data indexing. The process begins by partitioning the dataset into size-balanced subsets, which are then distributed across the available computational nodes. On each computing node, the lower level of the local index is built as follows. The assigned subset is randomly divided into groups of size g_1 . Each group is clustered independently, and for each resulting cluster, a set of representative prototypes is generated, effectively summarising the local data distribution. These prototypes constitute the first level of the local index on that node.

Once this level has been created, each set of representative prototypes is assembled with as many consecutive groups as needed to form a new group whose size is as close to g_1 as possible. These new groups are then clustered again to construct the next upper level of the hierarchy and this procedure is recursively applied until reaching a layer where the number of prototypes equals n_p . Once this process concludes, each computing node maintains an independent multilevel index, and the collection of all local structures constitutes the fully distributed index.

The structure generated by MSA depends on several index parameters:

- **Number of computing nodes** (n_{Nodes}). Defines the number of nodes over which the architecture is distributed, thereby controlling the level of parallelism and the degree of data partitioning. A larger n_{Nodes} results in smaller local subsets and lighter clustering and search workloads per node.
- **Group length** (g_1). Specifies the number of points processed together during each local clustering step. This parameter determines the batch size handled within each computing node and directly affects the computational cost of the local clustering procedure.
- **Number of prototypes per group** (n_p). Indicates how many representatives are selected from each group of size g_1 and promoted to the upper level of the hierarchy. Together with g_1 , this parameter determines the amount of information each group contributes to the upper levels, hence defining the structural granularity of the resulting index.
- **Clustering algorithm** (clusterAlg). The clustering algorithm is used to select the representative points from each group. The chosen method must partition the data space into Voronoi-like regions and identify a

prototype for each region. Since PDASC is compatible with a broad range of distance functions, the clustering algorithm must also support multiple dissimilarity measures. To this end, we instantiate this component using the classical k -medoids algorithm, whose prototype-based formulation naturally aligns with our hierarchical indexing strategy and ensures stable representatives (which, in this case, are real dataset elements) across diverse distance functions.

- **Distance function** (*distFunc*). A dissimilarity measure is chosen to compute the pairwise distances between dataset elements required by the clustering algorithm. The construction method generating the PDASC index is agnostic to the choice of distance function and independent of its underlying properties. The set of supported distances is determined by the selected clustering method, whose optimisation routines specify which dissimilarities can be handled efficiently. As the distance function directly influences prototype selection, it ultimately shapes the geometric structure of the resulting partitions.

Algorithm 1 Multilevel Structure Algorithm

```

1: procedure MSA(nNodes, dataset, gl, np, distFunc, clusterAlg)
2:   ▷ Split dataset into nNodes parts using a clustering algorithm
3:   dataList  $\leftarrow$  SPLIT(dataset, nNodes)
4:   nodeList  $\leftarrow$  []
5:   for node = 1, nNodes do
6:     data  $\leftarrow$  dataList[node]
7:     index  $\leftarrow$  CREATEINDEX(data, gl, np, distFunc, clusterAlg)
8:     nodeList.add(index)
9:   end for
10:  return nodeList
11: end procedure
12: procedure CREATEINDEX(data, gl, np, distFunc, clusterAlg)
13:   ▷ Divide dataset into nGroups groups of gl points
14:   vector, nGroups  $\leftarrow$  SPLIT(data, gl)
15:   ▷ Initialise multilevel structure
16:   levelPoints  $\leftarrow$  []
17:   idLevel  $\leftarrow$  0
18:   while nGroups  $\geq$  1 do
19:     ▷ Initialise auxiliary structures for each level
20:     groupsPoints, points  $\leftarrow$  []
21:     for idGroup = 1, nGroups do
22:       points  $\leftarrow$  vector[idGroup]
23:       groupsPoints.add(
24:         clustering(
25:           clusterAlg, distFunc, np, points))
26:     end for
27:     levelPoints.add(groupsPoints)
28:     vector, nGroups  $\leftarrow$  SPLIT(levelPoints, gl)
29:     idLevel += 1
30:   end while
31:   nLevels  $\leftarrow$  idLevel - 1
32:   return (levelPoints, nLevels)
33: end procedure

```

Fig. 1 illustrates an example of the index-building process of the MSA algorithm. In this example, a dataset of 320 elements is distributed across *nNodes* = 10 computing nodes, resulting in ten subsets of 32 elements each. For clarity, the figure only depicts the index construction performed on a single computing node.

The parameters are set to *gl* = 10 and *np* = 3, yielding a ratio of *np*/*gl* = 3/10. At the lowest level, the 32-element subset is partitioned into groups of size *gl*, producing three groups of 10 elements and a residual group of 2 elements. Each group is then clustered into *np* clusters (indicated by dashed circles), and one prototype is selected from each cluster and promoted to the next level.

At level 1, the prototypes produced by groups 0, 1, and 2 at level 0 are merged to form the first group of that layer. Generally, the algorithm combines the prototypes of a group with those of as many consecutive groups as needed to form a new group that is as close in size to *gl* as possible without exceeding its value. This procedure is applied recursively, producing progressively more compact prototype layers that summarise the level immediately below. The process concludes when a level containing exactly *np* points is formed (level 3 in this example).

The algorithm naturally handles variability in group sizes, a phenomenon particularly common in the lowest layers. When a group contains fewer than *np* elements, all of them are promoted. In this example, group 3 at level 0 contains only two elements, so both are promoted to level 1. Consequently, the group formed by the prototypes of groups 2 and 3 contains only five points, from which three prototypes are selected and promoted to the next level.

This procedure is executed independently on each of the *nNodes*, yielding a fully distributed hierarchical index.

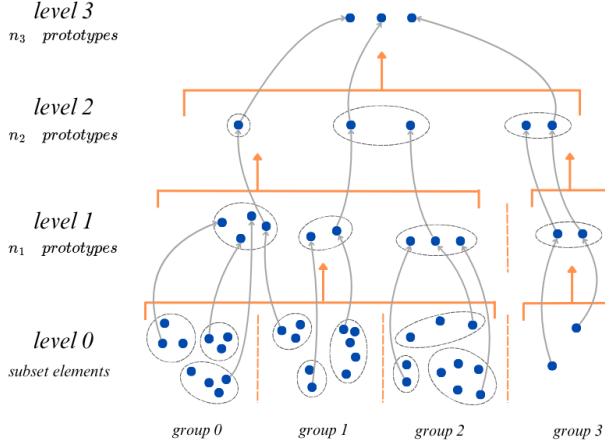


Figure 1: Conceptual representation of the multilevel index construction in PDASC using the MSA.

The NSA algorithm performs a top-down traversal of the multilevel index generated by the MSA on each computing node to efficiently retrieve candidates for the k -ANN of a query point q , as described in Algorithm 2. At each level, for every prototype selected for exploration, distances between q and its child prototypes (i.e. those associated with that prototype at the next lower level) are computed. Only the child prototypes whose distance to q is less than or equal to a predefined global radius r are selected for further exploration. The value of r can be determined based on measures that provide insight into the distribution of the dataset, such as the Cumulative Distribution Function or the maximum distance between elements. The level of restrictiveness can be adjusted according to the desired accuracy and available computational resources. This traversal continues recursively, progressively narrowing the search space until the bottom level is reached. At this lowest level, the corresponding data points are collected into the candidate pool. Once all computing nodes have completed their local traversals and calculated the distances from q to all candidates, such candidate sets are combined into a single pool. The final pool is then sorted to identify the top- k ANN (see Fig. 2).

Algorithm 2 Neighbours Search Algorithm (NSA)

```

1: procedure NSA(nodeList, distFunc, q, k, r)
2:   Candidates  $\leftarrow \emptyset$ 
3:   for each node in nodeList do
4:     idLevel  $\leftarrow$  getTopLevel(node)
5:     prototypes  $\leftarrow$  getPrototypes(node, idLevel)
6:     D  $\leftarrow$  distance(q, prototypes, distFunc)
7:     filteredPrototypes  $\leftarrow$  D  $\leq r$ 
8:     nodeCandidates  $\leftarrow$  EXPLORE CANDIDATES(filteredPrototypes, distFunc, q, r, idLevel - 1)
9:     D  $\leftarrow$  distance(q, nodeCandidates, distFunc)
10:    Candidates  $\leftarrow$  Candidates  $\cup$   $\{(c, d) \mid c \in \text{nodeCandidates}, d \in D\}$ 
11:   end for
12:   sortedCandidates  $\leftarrow$  sort(Candidates)
13:   neighbours  $\leftarrow$  sortedCandidates[0 : k]
14:   return neighbours
15: end procedure
16: procedure EXPLORE CANDIDATES(candidates, distFunc, q, r, idLevel)
17:   if idLevel = 0 then
18:     return candidates
19:   end if
20:   newCandidates  $\leftarrow \emptyset$ 
21:   for each candidate in candidates do
22:     mappedPoints  $\leftarrow$  getPrototypes(candidate, idLevel)
23:     D  $\leftarrow$  distance(q, mappedPoints, distFunc)
24:     filteredCandidates  $\leftarrow$  D  $\leq r$ 
25:     if filteredCandidates  $\neq \emptyset$  then
26:       result  $\leftarrow$  EXPLORE CANDIDATES(filteredCandidates, distFunc, q, r, idLevel - 1)
27:       newCandidates  $\leftarrow$  newCandidates  $\cup$   $\{result\}$ 
28:     end if
29:   end for
30:   return newCandidates
31: end procedure

```

Fig. 2 illustrates an example of the search process for retrieving the $3 - ANN$ of q . The global PDASC index is distributed across three computing nodes, each storing the portion of the index built from its local data partition. During query processing, NSA is executed independently on the index stored at each computing node. In the Figure, P_{x-y} denotes the y -th prototype at level x of the index located in a computing node, and p_{z-w} denotes the z -th data point in the subset located on computing node w . For clarity, the explanation focuses on the search performed on node 0; however, the described behaviour generalises to all other nodes.

The search process begins at the highest level of the index (level 3). NSA computes the distances between the query point q and all prototypes at this level (that is, $d(P_{3-0}, q)$, $d(P_{3-1}, q)$, etc.) and retains only those satisfying $d(q, P_{3-i}) \leq r$ for further exploration. In Fig. 2, prototypes that satisfy this condition and give rise to valid descent paths are represented by solid lines, whereas branches pruned due to distances exceeding the threshold are depicted with dotted lines. In the illustrated example, the prototypes P_{3-1} and P_{3-2} meet the threshold and are therefore explored at the next level.

The algorithm then evaluates the child prototypes mapped by each selected prototype, retaining only those that satisfy the distance condition. For example, P_{3-1} maps to *level 2* prototypes (P_{2-1}, P_{2-2}), but only P_{2-1} satisfies $d(q, P_{2-1}) \leq r$. The same behaviour occurs for the prototypes mapped by P_{3-2} .

Then, the algorithm continues recursively, expanding only the prototypes that meet the distance constraint. In this example, the valid descent paths from P_{2-1} and P_{2-3} lead to *level 1* prototypes $P_{1-1}, P_{1-3}, P_{1-7}$, and P_{1-11} , from which the search eventually reaches the corresponding points at *level 0*. These points constitute the candidate set retrieved on *node 0*, which is then merged with the candidates obtained from *node 1* and *node 2*.

After merging, all candidate points are globally sorted by their distance to q , and the three closest points are selected as the final nearest neighbours. In this example, the 3 -ANN returned by the search are:

$$3\text{-ANN} = \{ p_{0-4}, p_{1-8}, p_{0-14} \}.$$

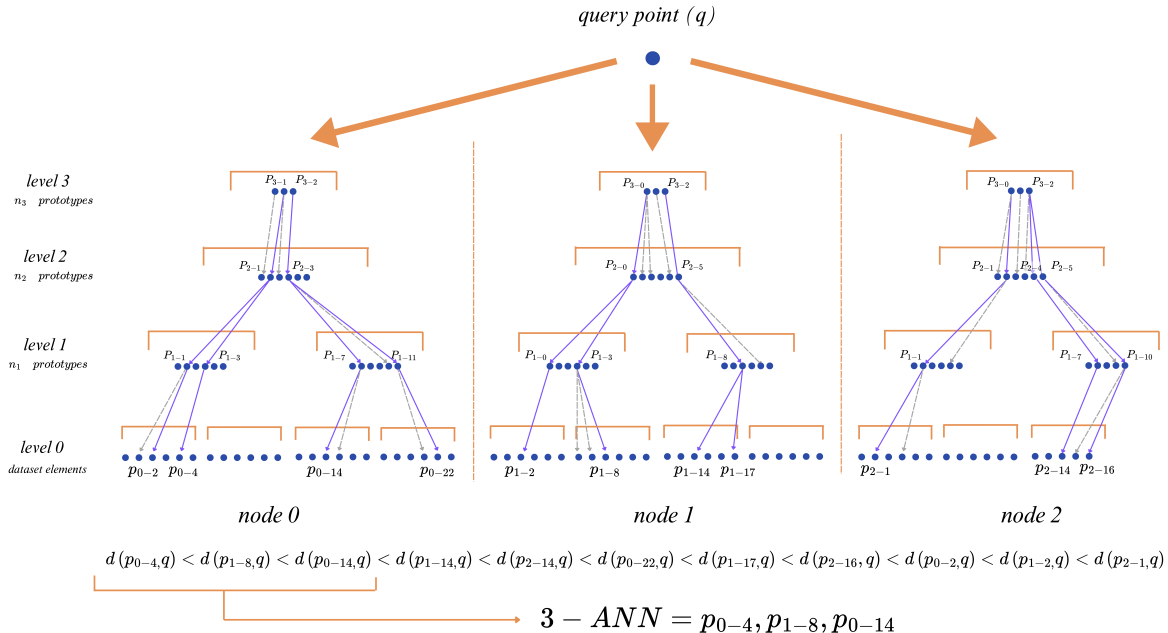


Figure 2: Conceptual illustration of the k -NN search in PDASC using the NSA over a multilevel index distributed across $nNodes = 3$ computing nodes. The dataset of 65 elements is partitioned into subsets of 24 (node 0), 24 (node 1), and 11 elements (node 2), where each local index is built using $gl = 6$ and $np = 3$.

3.2 IMPACT OF THE INDEX PARAMETERS

The topology and configuration of the PDASC index structure are governed by the parameters introduced in Section 3.1 and, crucially, by the relationships among some of them. This topology, in turn, influences multiple performance aspects, including recall, NDC and index size. Beyond the qualitative insights discussed below, the observations are supported by the experimental results reported in Section 4.

Number of computing nodes (`nNodes`). As discussed in Section 3.1, increasing `nNodes` enhances parallelism and reduces the local workload per node. Experimentally, this improves computational efficiency during search and reduces per-node index size. However, these gains exhibit a diminishing returns pattern: beyond a certain point, adding more nodes yields progressively smaller improvements due to an increasingly fragmented data space.

Group length (`g1`). The influence of `g1` is primarily indirect. Small values generate many small groups, increasing clustering overhead, whereas very large values raise the internal cost of clustering within each group. Although its isolated effect on recall and NDC is moderate, `g1` does play a central role in shaping the index topology through its interaction with `np`. Experimental results across datasets with different densities confirm that the optimal value of `g1` is data-dependent.

Number of prototypes per group (`np`). Larger values of `np` increase index size and indexing time by propagating more representatives to higher levels of the hierarchy. Yet, when considered alone, the effect of `np` on recall and NDC is limited. Most of its performance influence arises through its interaction with `g1`, as the number of prototypes is meaningful only relative to the size of the group from which they are selected.

Prototype-to-group ratio (`np/g1`). This ratio is the dominant factor determining the resulting index topology and, consequently, recall and NDC. Low ratios produce compact hierarchies and increase the proportion of the index explored during search, yielding high recall at the cost of higher NDC (indeed, extremely low ratios approach full-scan behaviour). Conversely, high ratios generate overly dense upper layers in which too many representatives are propagated, leading to excessive partitioning and less faithful cluster representations. As a consequence, pruning decisions occur prematurely, since the upper-level structure does not accurately reflect the underlying data distribution, ultimately reducing recall. As a result, the index size increases with the ratio, as more prototypes are propagated upward through the hierarchy. Therefore, effective index construction requires a balanced ratio that ensures sufficient coverage of the search space without incurring over-partitioning.

4 EXPERIMENTAL STUDY

This section presents a comprehensive empirical evaluation of PDASC. Experiments are conducted on the datasets listed in Table 1, selecting distance functions that reflect the semantic notion of similarity inherent to each dataset while assessing PDASC’s support for arbitrary dissimilarity measures.

The evaluation is organised into two parts. First, we analyse how different parametrisations shape the hierarchical index structure, influencing its topology, size, and the behaviour of the search algorithm. Second, we compare PDASC against state-of-the-art ANN algorithms to contextualise its performance, in terms of both computational cost and memory footprint.

For quality assessment, we report the recall achieved under different parametrisations, measured against the ground-truth set of 10-NN obtained via exact search. For performance assessment, we evaluate both the NDC per computing node and the index size stored on each node.

As distance evaluations constitute the dominant component of query-time cost in most ANN algorithms [32, 33], NDC is adopted as the primary performance metric. Moreover, it helps isolate the intrinsic behaviour of the algorithm by reducing the influence of platform-dependent optimisations (such as low-level SIMD vectorisation, cache-aware memory layouts, or multi-threading strategies) that may otherwise bias comparisons, even within the same architecture, thereby providing a clearer view of the underlying computational cost.

Similarly, index size has been included as a complementary metric, as memory footprint is a critical limiting factor in large-scale ANN systems and becomes even more relevant in low-resource and distributed environments. In such scenarios, index size determines RAM usage, persistent storage requirements, and even the number of machines needed to host the system, directly impacting operational and energy costs. Considering index size, therefore, provides a realistic assessment of scalability and practical viability in distributed infrastructures.

Thus, we will examine how NDC and index size per computing node vary across different parameter settings, presenting recall–NDC and recall–index-size trade-off plots that characterise the relationship between accuracy, computational effort, and memory footprint [34, 35].

All experiments were conducted on a server equipped with an AMD EPYC Genoa processor (32 cores / 64 threads, 3.25 GHz, 256 MB L3 cache, 280 W, SP5 socket, UP), 12 × 32GB DDR5 4800MHz ECC registered RAM, and six Micron 5400Pro SSDs (960GB, 2.5" SATA 6Gb/s) for secondary storage.

4.1 DATASETS

Table 1 lists the five publicly available datasets used in our experiments, which differ in their type, number of elements (n), and dimensionality (D). Four of these datasets (MNIST, NYTimes, GLOVE, and MovieLens-10M) are standard benchmarks commonly used to evaluate ANN search implementations [12], ensuring comparability with prior work. The *Municipalities* dataset is a two-dimensional geospatial collection comprising the latitude and longitude coordinates of all 8,130 municipalities in Spain². Hence, this is a representative test case for geospatial queries, allowing the use of the Haversine distance function [36] to further enrich the diversity of distance measures considered in the experimental study. These datasets also exhibit various levels of local intrinsic dimensionality (LID) [37], confirming the variety and difficulty of our evaluation scenarios [34] and are processed using different distance functions to assess PDASC’s support for arbitrary distances, including common metric distances (e.g., Euclidean), less frequently used ones (e.g., Jaccard), and non-metric distances (e.g., cosine).

Table 1: Summary of key features of selected datasets.

Dataset	n	D	Data Type	LID	Distance
<i>Municipalities</i>	8,130	2	Geospatial	2.65	Haversine
MNIST	69,000	784	Image	13.05	Euclidean
GLOVE	10^6	100	Text	17.62	Cosine
NYTimes	290,000	256	Text	46.88	Cosine
MovieLens10M	65,134	69,363	Boolean	22.41	Jaccard

4.2 STRUCTURAL SENSITIVITY ANALYSIS OF PDASC

The PDASC algorithm was entirely implemented in Python³. For the k -medoids clustering, it relies on the `FastPAM` Python implementation [38], chosen for its high computational efficiency and support for a broad variety of distance measures, which ensures compatibility with the diverse dissimilarity functions employed in our experiments.

For each dataset, the data is randomly split into non-overlapping training and test subsets to ensure statistical robustness and avoid bias. The training sets are then partitioned and distributed across $nNodes$ computational nodes. In this study, we evaluate configurations with $nNodes \in \{1, 3, 5, 10\}$ to illustrate different levels of parallelism and demonstrate PDASC’s applicability in distributed environments. At each computational node, an index tree is constructed by applying the MSA algorithm to the corresponding subset, using the selected clustering algorithm, distance function, group length ($g1$), and number of prototype points (np). To assess index structures at different levels of granularity, we evaluate several $np/g1$ ratios, specifically 0.02, 0.05, 0.1, 0.2, 0.33, and 0.5.

Subsequently, the 10-ANN search for each query point (q) in the test set is performed using NSA. The radius parameter (r) is selected according to the dataset distribution and the desired search quality. For each experiment, different values of r are tested to explore varying levels of restrictiveness.

Fig. 3a illustrates how the recall–NDC trade-off per computing node evolves under different PDASC configurations on the GLOVE dataset. Markers sharing the same colour correspond to the same search radius and number of computing nodes. Within each colour group, different data points correspond to different $np/g1$ ratios, thus inducing distinct index topologies. As expected, increasing the number of computing nodes reduces the per-node computational effort, although efficiency gains diminish beyond a certain point. Moreover, larger search radii consistently yield higher recall, generally at the expense of increased NDC. Importantly, this chart also reveals that, even with a sufficient number of computing nodes and an appropriately chosen search radius, the overall performance of the algorithm remains strongly dependent on the index configuration, particularly on the choice of the np and $g1$ parameters, whose impact is analysed in more detail in the following figure.

Fig. 3b reports the same experimental setting but fixes the search radius to the most restrictive value, $r = 0.91$, in order to isolate and accentuate the influence of the $np/g1$ ratio under stringent search conditions. While it is evident that $nNodes$ and the search radius influence the per-node NDC–recall balance, the $np/g1$ ratio plays a critical role in determining how effectively the hierarchy represents the data, thereby influencing this trade-off. Very large ratios lead to an overly coarse representation, resulting in both low recall and low NDC. As the ratio decreases, prototypes capture local structure more faithfully, yielding a rapid increase in recall at a relatively modest computational cost. Further

²<https://ign.es/web/rcc-nomenclator-nacional>

³All code related to the proposed algorithm and the implementation of experiments is hosted in the elenagarciamorato/PDASC GitHub repository.

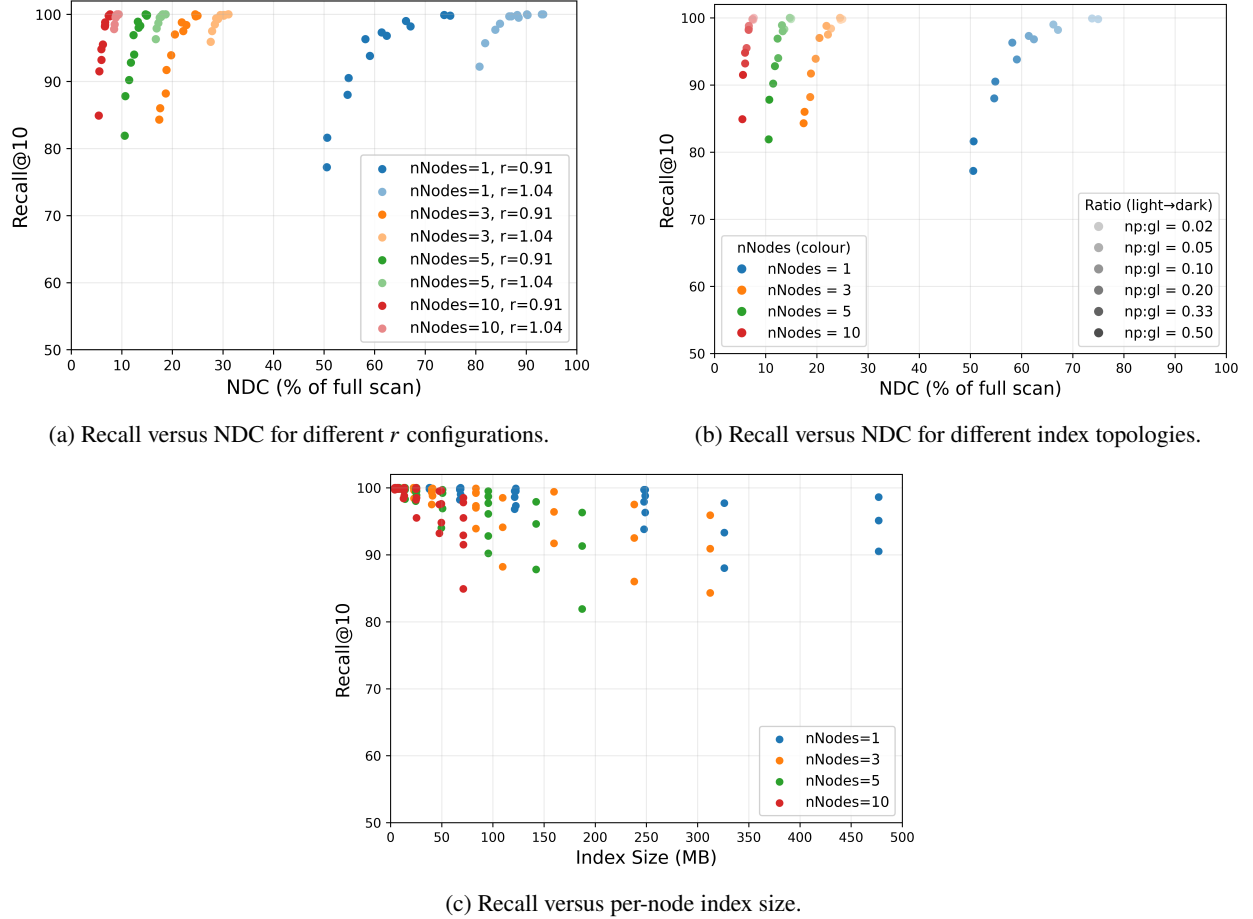


Figure 3: PDASC Performance on GLOVE dataset under different degrees of parallelisation ($nNodes$).

reductions eventually lead to over-exploration of the hierarchy, as reflected by a steep rise in NDC with only marginal gains in recall. Across all evaluated datasets, intermediate $np/g1$ ratios, typically around 0.2–0.3, consistently provide the most favourable balance among recall, NDC, and index size. These ratios achieve recall values above 90% while maintaining substantially reduced computational costs and moderate memory requirements.

Fig. 3c reports the memory footprint of PDASC at each computing node as a function of the number of $nNodes$ employed. While it is evident that the index size is largely governed by the $nNodes$ parameter (increasing $nNodes$ spreads the load and reduces both the per-node and overall memory footprint), certain configurations with fewer nodes achieve comparable or even higher recall (upper-left part of the figure). This is again due to the $np/g1$ ratio, since the index topology not only determines index size but, more importantly, search effectiveness, thereby impacting the trade-off between recall and efficiency.

Overall, the empirical evaluation validates the theoretical characterisation of PDASC presented in Section 3.2: the index topology induced by $nNodes$ and the $np/g1$ ratio governs memory distribution and representativeness, ultimately determining the trade-offs between computational efficiency, pruning behaviour, and search accuracy.

4.3 BENCHMARKING WITH ALTERNATIVE ANN ALGORITHMS

Finally, empirical results are compared against selected state-of-the-art algorithms. Benchmarking ANN methods is inherently challenging due to the continuous evolution of algorithms and implementations. Therefore, in this study, we include well-established and widely used approaches from different ANN families, all available through Python implementations: ANNOY, PyNNDescent, the FAISS [39] implementations of LSH and IVF and the Python bindings of the HNSW implementation from nmslib [40].

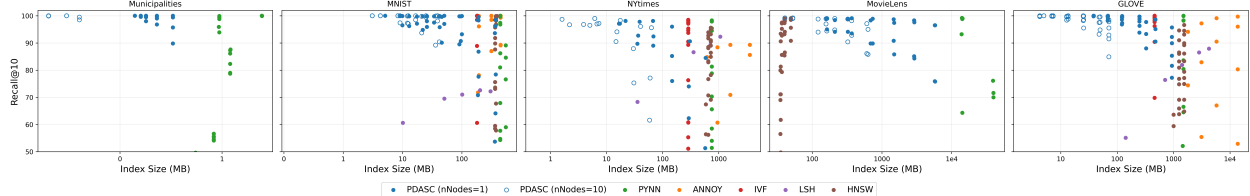


Figure 4: Per-node index size versus recall for PDASC and the evaluated ANN methods across all datasets (x-axis in logarithmic scale).

Fig. 4 presents, for all datasets considered in this study, the per-node index size–recall profiles of the selected SOTA methods under different parameter settings, together with the PDASC configurations for $n\text{Nodes}=1$ and $n\text{Nodes}=10$, which represent the most extreme cases evaluated, ranging from a fully centralised index to a highly distributed deployment. Notably, only PyNNDescent, HNSW, and PDASC are compatible with MovieLens-10M, while only PDASC and PyNNDescent support the *Municipalities* dataset, due to the use of Jaccard and Haversine distances respectively, metrics unsupported by most conventional ANN frameworks.

This figure illustrates not only the search quality achieved by different methods but also how efficiently each method uses the available resources at node level, revealing distinct behaviours across algorithms. Methods such as HNSW and IVF exhibit an almost constant per-node index size, whereas their recall varies depending on their internal configuration. Conversely, ANNOY and PyNNDescent exhibit greater variability in memory footprint while attaining a broad range of recall levels regardless of index sizes. LSH shows the greatest variability in memory footprint across parameter settings and is also the method that consistently delivers substantially lower recall. Across all datasets, the PDASC index remains smaller than, or comparable in size to, all evaluated methods at equivalent recall levels, even when the entire PDASC index is concentrated on a single node, thereby highlighting its memory-efficient design.

Regarding the NDC–recall benchmarking, only PDASC and IVF explicitly report NDC values, enabling their performance to be characterised through recall–NDC trade-offs. The remaining methods do not provide distance-computation statistics, precluding an assessment of their intrinsic computational cost via implementation-independent metrics. Fig. 5 illustrates this comparison.

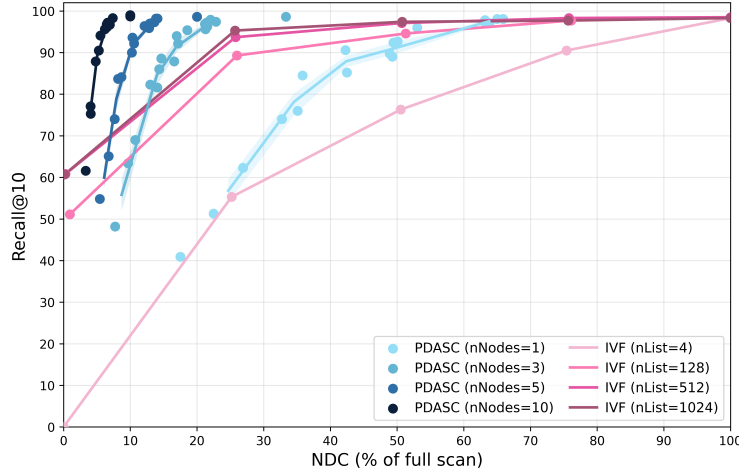


Figure 5: Recall versus NDC for PDASC and IVF on the NYTimes dataset.

For IVF, each line in the plot corresponds to a different $n\text{list}$ configuration, while points along each line represent increasing values of $n\text{probe}$, fixed at 0%, 25%, 50%, 75%, and 100% of the selected $n\text{list}$. For PDASC, each line corresponds to a different $n\text{nodes}$ setting, and each point denotes a distinct $n\text{p}/g\text{l}$ ratio, inducing a different index topology.

The results indicate that, for comparable recall levels, PDASC requires significantly fewer distance computations per node than IVF. In PDASC, increasing the number of computing nodes $n\text{Nodes}$ effectively shifts the operational curves toward the left of the spectrum, demonstrating that as the algorithm better exploits its parallelisation capability, the recall–NDC trade-off improves. Conversely, IVF shows a wider dispersion and higher local computational demand to

reach equivalent accuracy. This comparison highlights PDASC’s ability to maintain high search quality while keeping local resource requirements low, making it particularly suitable for environments where per-node computational power is a constraint.

5 CONCLUSIONS AND FUTURE WORK

This paper presented PDASC, a distributed ANN search algorithm whose core contribution lies in a flexible index design that simultaneously addresses several fundamental challenges of modern similarity search. PDASC relies on a single hierarchical index structure whose properties naturally support arbitrary distance functions and enable efficient deployment in distributed, memory-constrained environments. The proposed hierarchical clustering-based index leverages dense local representations to mitigate practical manifestations of the curse of dimensionality, preserving informative neighbourhood structure even when global distance contrast collapses.

PDASC is designed to operate under arbitrary dissimilarity measures without relying on metric assumptions that constrain many existing ANN methods. This capability is not introduced as a separate mechanism, but emerges from the distance-agnostic nature of the index construction and traversal strategy, which decouples indexing and exploration from specific distance properties. As a result, PDASC supports non-metric and domain-specific similarities, enabling similarity search in heterogeneous and high-dimensional data spaces.

The same structural principles that enable distance-function flexibility also allow to efficiently deploy PDASC in distributed and low-resource environments. The index naturally partitions both storage and search across multiple computing nodes, avoiding centralised structures and eliminating reliance on specialised hardware acceleration. This design enables PDASC to operate within limited storage budgets while scaling effectively on commodity hardware.

Through an extensive structural sensitivity analysis, we showed that the resulting index topology, largely governed by the prototype-to-group ratio and the number of computing nodes, directly controls the trade-off among recall, computational cost, and memory footprint. Empirical results across diverse datasets and distance functions demonstrate that PDASC consistently achieves competitive recall while requiring a smaller or comparable per-node index size than state-of-the-art ANN methods. When distance computations are explicitly measured, PDASC attains favourable accuracy–efficiency trade-offs without relying on GPUs, TPUs, or other specialised hardware accelerators. By limiting memory usage per node and avoiding hardware-intensive optimisations, PDASC reduces computational overhead and energy consumption, making it well-suited for resource-aware and energy-conscious deployments.

Overall, PDASC addresses a practical gap in the ANN landscape by enabling similarity search in heterogeneous, high-dimensional, and memory-constrained environments, where many existing methods are inapplicable. Its combination of distance-function flexibility, distributed execution, and low memory footprint offers a viable solution for large-scale systems that prioritise scalability, accessibility, and environmentally responsible computing.

Several opportunities exist for further refinement and research. A key direction is to improve the computational efficiency of the current implementation, for example, by porting PDASC to a high-performance language such as Rust⁴ or Go⁵. Another promising direction concerns the role of the search radius, as preliminary observations indicate that its value can significantly influence performance. Identifying an optimal radius at each index level, according to the local data distribution, may enable PDASC to better leverage its inherent ability to adapt to heterogeneous densities and structural variations within the dataset. Additionally, future work could focus on improving the selection of representative points to construct the hierarchical structure, for instance, by incorporating core-set techniques that capture the underlying data distribution more accurately.

References

- [1] Edgar Chávez, Gonzalo Navarro, Ricardo Baeza-Yates, and José Luis Marroquín. Searching in Metric Spaces. *ACM Comput. Surv.*, 33(3):273–321, September 2001. ISSN 0360-0300. doi:10.1145/502807.502808.
- [2] Hanan Samet. *Foundations of Multidimensional and Metric Data Structures*. The Morgan Kaufmann Series in Data Management Systems. Academic Press, San Francisco, CA, USA, 2006. ISBN 978-0-12-369446-1.
- [3] Pavel Zezula, Giuseppe Amato, Vlastislav Dohnal, and Michal Batko. *Similarity Search - The Metric Space Approach*, volume 32 of *Advances in Database Systems*. Springer, New York, NY, 2006. ISBN 978-0-387-29146-8. doi:10.1007/0-387-29151-2.

⁴<https://rust-lang.org/>

⁵<https://go.dev>

[4] Ricardo Baeza-Yates and Berthier Ribeiro-Neto. *Modern Information Retrieval: The Concepts and Technology Behind Search*. Pearson Education Ltd., Harlow, England, 2 edition, 2011. ISBN 978-0-321-41691-9. URL <http://www.mir2ed.org/>.

[5] Rahel Arnold, Werner Bailer, Ralph Gasser, Björn P. Jónsson, Omar Shahbaz Khan, Heiko Schuldt, Florian Spiess, and Lucia Vadicamo. Multimedia information retrieval in xr. In *Proceedings of the 32nd ACM International Conference on Multimedia*, MM '24, page 11285–11286, New York, NY, USA, 2024. Association for Computing Machinery. ISBN 9798400706868. doi:10.1145/3664647.3689176.

[6] Hamed Zamani, Fernando Diaz, Mostafa Dehghani, Donald Metzler, and Michael Bendersky. Retrieval-enhanced machine learning. In *Proceedings of the 45th International ACM SIGIR Conference on Research and Development in Information Retrieval*, SIGIR '22, page 2875–2886, New York, NY, USA, 2022. Association for Computing Machinery. ISBN 9781450387323. doi:10.1145/3477495.3531722.

[7] Michel Van Kempen, Stephanie S Kim, Charlotte Tumescheit, Milot Mirdita, Jeongjae Lee, Cameron LM Gilchrist, Johannes Söding, and Martin Steinegger. Fast and accurate protein structure search with Foldseek. *Nat. Biotechnol.*, 42(2):243–246, 2024. doi:10.1038/s41587-023-01773-0.

[8] Siyuan Shang, Xuehui Du, Xiaohan Wang, and Aodi Liu. Private approximate nearest neighbor search for on-chain data based on locality-sensitive hashing. *Futur. Gener. Comput. Syst.*, 164:107586, 2025. ISSN 0167-739X. doi:<https://doi.org/10.1016/j.future.2024.107586>.

[9] Christian Böhm, Stefan Berchtold, and Daniel A. Keim. Searching in High-Dimensional Spaces: Index Structures for Improving the Performance of Multimedia Databases. *ACM Comput. Surv.*, 33(3):322–373, September 2001. ISSN 0360-0300. doi:10.1145/502807.502809.

[10] Sergey Shvydun. Models of similarity in complex networks. *PeerJ Comput. Sci.*, 9:e1371, May 2023. ISSN 2376-5992. doi:10.7717/peerj-cs.1371.

[11] Rezvan Ehsani and Finn Drabløs. Robust Distance Measures for k NN Classification of Cancer Data. *Cancer Informat.*, 19:117693512096554, 1 2020. ISSN 1176-9351, 1176-9351. doi:10.1177/1176935120965542.

[12] Martin Aumüller, Erik Bernhardsson, and Alexander Faithfull. ANN-Benchmarks: A benchmarking tool for approximate nearest neighbor algorithms. *Inf. Syst.*, 87:101374, 2020. ISSN 0306-4379. doi:10.1016/j.is.2019.02.006.

[13] David W. Scott and J. R. Thompson. Probability density estimation in higher dimensions. In J. E. Gentle, editor, *Computer Science and Statistics: Proceedings of the Fifteenth Symposium on the Interface*, pages 173–179, 1983.

[14] Roger Weber, Hans-Jörg Schek, and Stephen Blott. A Quantitative Analysis and Performance Study for Similarity-Search Methods in High-Dimensional Spaces. In Ashish Gupta, Oded Shmueli, and Jennifer Widom, editors, *Proceedings of the 24rd International Conference on Very Large Data Bases, VLDB'98, August 24-27, 1998, New York City, New York, USA*, pages 194–205. Morgan Kaufmann, 1998. URL <http://www.vldb.org/conf/1998/p194.pdf>.

[15] Zeyu Wang, Peng Wang, Themis Palpanas, and Wei Wang. Graph- and tree-based indexes for high-dimensional vector similarity search: Analyses, comparisons, and future directions. *IEEE Data Eng. Bull.*, 46(3):3–21, 2023. URL <http://sites.computer.org/debull/A23sept/p3.pdf>.

[16] Yury A. Malkov and Dmitry A. Yashunin. Efficient and Robust Approximate Nearest Neighbor Search Using Hierarchical Navigable Small World Graphs. *IEEE Trans. Pattern Anal. Mach. Intell.*, 42(4):824–836, 2020. doi:10.1109/TPAMI.2018.2889473.

[17] Mengzhao Wang, Xiaoliang Xu, Qiang Yue, and Yuxiang Wang. A comprehensive survey and experimental comparison of graph-based approximate nearest neighbor search. *Proc. VLDB Endow.*, 14(11):1964–1978, 2021. doi:10.14778/3476249.3476255.

[18] Vladimir Mic, David Novak, and Pavel Zezula. Binary sketches for secondary filtering. *ACM Trans. Inf. Syst.*, 37(1):1–28, 2018. doi:10.1145/3231936.

[19] Xi Zhao, Yao Tian, Kai Huang, Bolong Zheng, and Xiaofang Zhou. Towards efficient index construction and approximate nearest neighbor search in high-dimensional spaces. *Proc. VLDB Endow.*, 16(8), 2023. ISSN 2150-8097. doi:10.14778/3594512.3594527. URL <https://doi.org/10.14778/3594512.3594527>.

[20] Edgar Chávez and Gonzalo Navarro. A compact space decomposition for effective metric indexing. *Pattern Recognit. Lett.*, 26(9):1363–1376, 2005. ISSN 0167-8655. doi:<https://doi.org/10.1016/j.patrec.2004.11.014>.

[21] Jeff Johnson, Matthijs Douze, and Hervé Jégou. Billion-scale similarity search with GPUs. *IEEE Trans. Big Data*, 7(3):535–547, 2019. doi:10.1109/TBDA.2019.2921572.

[22] Donna Xu, Ivor W. Tsang, and Ying Zhang. Online product quantization. *IEEE Trans. on Knowl. and Data Eng.*, 30(11), 2018. ISSN 1041-4347. doi:10.1109/TKDE.2018.2817526. URL <https://doi.org/10.1109/TKDE.2018.2817526>.

[23] Giuseppe Amato, Fabrizio Falchi, Fausto Rabitti, and Lucia Vadicamo. Some Theoretical and Experimental Observations on Permutation Spaces and Similarity Search. In *Similarity Search and Applications - 7th International Conference, SISAP 2014, Los Cabos, Mexico, October 29-31, 2014. Proceedings*, volume 8821 of *Lecture Notes in Computer Science*, pages 37–49. Springer, 2014. doi:10.1007/978-3-319-11988-5_4.

[24] Edgar Chávez, Karina Figueroa, and Gonzalo Navarro. Effective proximity retrieval by ordering permutations. *IEEE Trans. Pattern Anal. Mach. Intell.*, 30(9):1647–1658, 2008. doi:10.1109/TPAMI.2007.70815.

[25] Matej Antol, Jaroslav Ol'ha, Terézia Slanináková, and Vlastislav Dohnal. Learned Metric Index—Proposition of learned indexing for unstructured data. *Inf. Syst.*, 100:101774, 2021. ISSN 0306-4379. doi:10.1016/j.is.2021.101774.

[26] Tim Kraska, Alex Beutel, Ed H. Chi, Jeffrey Dean, and Neoklis Polyzotis. The Case for Learned Index Structures. In *Proceedings of the 2018 International Conference on Management of Data, SIGMOD '18, Houston, TX, USA, June 10–15, 2018*, page 489–504, New York, NY, USA, 2018. Association for Computing Machinery. ISBN 9781450347037. doi:10.1145/3183713.3196909.

[27] Piotr Indyk and Rajeev Motwani. Approximate nearest neighbors: towards removing the curse of dimensionality. In *Proceedings of the thirtieth annual ACM symposium on Theory of computing - STOC '98*, pages 604–613, Dallas, Texas, United States, 1998. ACM Press. ISBN 978-0-89791-962-3. doi:10.1145/276698.276876.

[28] Kevin Beyer, Jonathan Goldstein, Raghu Ramakrishnan, and Uri Shaft. When Is “Nearest Neighbor” Meaningful? In Catriel Beeri and Peter Buneman, editors, *Database Theory — ICDT'99*, volume 1540 of *Lecture Notes in Computer Science*, pages 217–235. Springer, Berlin, Heidelberg, 1 1999. ISBN 978-3-540-49257-3. doi:10.1007/3-540-49257-7_15.

[29] Wen Li, Ying Zhang, Yifang Sun, Wei Wang, Mingjie Li, Wenjie Zhang, and Xuemin Lin. Approximate Nearest Neighbor Search on High Dimensional Data — Experiments, Analyses, and Improvement. *IEEE Trans. Knowl. Data Eng.*, 32(8):1475–1488, 2020. doi:10.1109/TKDE.2019.2909204.

[30] Yiwei Pan, Zhibin Pan, Yikun Wang, and Wei Wang. A new fast search algorithm for exact k-nearest neighbors based on optimal triangle-inequality-based check strategy. *Knowl.-Based Syst.*, 189:105088, 2020. ISSN 0950-7051. doi:https://doi.org/10.1016/j.knosys.2019.105088. URL <https://www.sciencedirect.com/science/article/pii/S0950705119304678>.

[31] Vladimir Pestov. Indexability, concentration, and vc theory. In *Proceedings of the Third International Conference on SImilarity Search and APplications, SISAP '10*, page 3–12, New York, NY, USA, 2010. Association for Computing Machinery. ISBN 9781450304207. doi:10.1145/1862344.1862346. URL <https://doi.org/10.1145/1862344.1862346>.

[32] Jianyang Gao and Cheng Long. High-dimensional approximate nearest neighbor search: with reliable and efficient distance comparison operations. *Proc. ACM Manag. Data*, 1(2), June 2023. doi:10.1145/3589282.

[33] Yun Peng, Byron Choi, Tszi Nam Chan, Jianye Yang, and Jianliang Xu. Efficient approximate nearest neighbor search in multi-dimensional databases. *Proc. ACM Manag. Data*, 1(1), May 2023. doi:10.1145/3588908.

[34] Martin Aumüller and Matteo Ceccarello. The role of local dimensionality measures in benchmarking nearest neighbor search. *Inf. Syst.*, 101:101807, 2021. ISSN 0306-4379. doi:10.1016/j.is.2021.101807.

[35] Mingyu Yang, Wentao Li, Jiabao Jin, Xiaoyao Zhong, Xiangyu Wang, Zhitao Shen, Wei Jia, and Wei Wang. Effective and general distance computation for approximate nearest neighbor search, 2025. URL <https://arxiv.org/abs/2404.16322>.

[36] Roger W. Sinnott. Virtues of the haversine. *Sky Telesc.*, 68(2):159, 1984.

[37] Michael E Houle. Dimensionality, discriminability, density and distance distributions. In *2013 IEEE 13th International Conference on Data Mining Workshops*, pages 468–473. IEEE, 2013. doi:10.1109/ICDMW.2013.139.

[38] Erich Schubert and Lars Lenssen. Fast k-medoids Clustering in Rust and Python. *J. Open Source Softw.*, 7(75):4183, 7 2022. ISSN 2475-9066. doi:10.21105/joss.04183.

[39] Matthijs Douze, Alexandre Guzhva, Chengqi Deng, Jeff Johnson, Gergely Szilvassy, Pierre-Emmanuel Mazaré, Maria Lomeli, Lucas Hosseini, and Hervé Jégou. The faiss library, 2025. URL <https://arxiv.org/abs/2401.08281>.

[40] Yu A Malkov and D A Yashunin. Efficient and robust approximate nearest neighbor search using hierarchical navigable small world graphs. *IEEE Trans. Pattern Anal. Mach. Intell.*, 42(4):824–836, 2020.